

Water yield forecast in Shandong Province based on InVEST model

Yushan Li ^{1, 2, 3, a}, Huawei Chen ^{2, 3, b, *}, Fulin Li ^{2, 3, c}, Long Jiang ^{4, d, *},
 Jian Zhang ^{5, e}

¹ School of Water Conservancy and Environment, University of Jinan, Jinan 250022, China;

² Key Laboratory of Water Resources and Environment of Shandong Province, Jinan 250014, China;

³ Water Resource Research Institute of Shandong Province, Jinan 250014, China;

⁴ Yantai Hydrology and Water Resources Investigation Center, Yantai 265500, China;

⁵ Shandong Institute of Petroleum and Chemical Technology, Dongying 257100, China

^a 870597187@qq.com, ^b chenhuawei8036@163.com, ^c fulinli@126.com, ^d 103058734@qq.com,
^e 1768174746@qq.com

Abstract. A better understanding of the effects of land use change and climate change on water yield is highly important for water resource planning and sustainable management. Land use changes in Shandong Province were analyzed over recent years. The PLUS Model was applied to forecast the land use layout for 2032, with adjustments made based on actual conditions and utilizing various CMIP6 scenarios for precipitation and actual evapotranspiration. The 2032 Water Yield was quantified using the InVEST Model at both grid and administrative scales, and its temporal-spatial characteristics and spatial correlation were analyzed. The findings revealed several key points: first, a decrease of 16.92% in arable land area, along with diminishing trends in grassland and unused land, and an increase of 33.92% in built-up land area, accompanied by growth in forest and water area. Second, the water yield decreases from southeast to northwest in Shandong Province, with significant inter-annual variations. Third, future predictions suggest that the annual water yield generally increases during flat water years, with offshore areas exhibiting greater water yield depth compared to inland areas. Rizhao is projected to have the highest water yield depth, while Binzhou and Dongying are expected to have the lowest depths, with a spatially positive correlation between them.

Keywords: Land use; water yield; InVEST model; Shandong province.

1. Introduction

Shandong Province is a major agricultural province with water scarcity. The spatial and temporal allocation of water resources is imbalanced and fails to align with the irrigation needs of agricultural fields. There are also drastic changes within and between years, and the irrigation guarantee rate of local water resources is not high. [1] Beginning with the "14th Five-Year Plan," Shandong Province has consistently embraced the "three water coordination" approach, encompassing the management of water resources, environmental water concerns, and water-related ecosystems, actively pursuing the enhancement of water ecological standards. Nonetheless, the underlying ecological demands for water in its rivers and lakes remain inadequately met, with a pronounced scarcity in water resources persisting. Many pressures, such as uneven spatial and temporal distribution, have not been alleviated. Quantitative assessment and prediction of water yield functions in Shandong Province can help formulate effective water resources management strategies and protect and restore ecosystem functions.

The Integrated Valuation of Ecosystem Services and Tradeoffs (InVEST) approach is a prevalent model for appraising ecosystem services, capable of quantifying ecological and hydrological dynamics across extensive land areas. Its module for calculating water production operates on a grid-level basis. The water balance estimation method is influenced by changes in precipitation, actual

surface evapotranspiration, soil moisture conditions and land use types in the hydrological cycle.[2][3]The impact of land utilization on the uneven distribution of water production across different areas is intricate. Variations in land use alter the fundamental characteristics of the surface, which include soil texture, ground unevenness, albedo, the local cycle of water vapor, and surface water flow, among other factors. Hydrological processes affect regional actual evapotranspiration and precipitation, especially actual evapotranspiration, which in turn affects water yield.[4][5]

Water yield affects the overall level of regional water resources, and imbalances in water yield will limit the sustainable development of regional economies. The research zeroes in on Shandong Province's bureaucratic sectors and scrutinizes the evolving patterns, areal disparities, and shifts in water production utilizing the InVEST framework. It aims to forecast forthcoming water production potential while examining its geographical variations, spatial clustering, and additional influencers. This study shall furnish empirical support for the governance of water resources and bolster sustainable growth within the region.

2. Overview of the study area

Nestled along China's eastern seaboard and situated downstream of the Yellow River, Shandong Province spans from 34°22'N to 38°23'N latitude and from 114°45'E to 122°42'E longitude. Covering 158,000 square kilometers, the region administers 16 cities at the prefecture level and is home to over 100 million inhabitants. Approximately 59% of Shandong's topography is comprised of mountainous and hilly landscapes. Elevated terrain consisting of hills and minor mountains spans the eastern region, whereas the central territory is also characterized by similar elevated landscapes, with a basin occupying the western sector. Predominant waterways include the Huaihe, Haihe, and chiefly the Yellow River—the latter being the most significant in Shandong Province. Water resources across Shandong vary notably, with the eastern seaboard boasting a comparative abundance and the inland central to western regions facing a scarcity. The province is home to a total of 675 water storage facilities, which together can hold up to 26.22 billion cubic meters, featuring 16 vast reservoirs, 26 of moderate size, and 633 of a smaller scale. Regarding the variety of land utilization, Shandong Province exhibits a wide array of features. The most recent data indicates that Shandong Province encompasses 640 million acres of agricultural fields, 93 million acres dedicated to horticulture, 270 million acres of woodland, 37 million acres of pasture, and 190 million acres allocated for urban, residential, industrial, and mining purposes. Additionally, the province includes 34 million acres used for transport infrastructure and an equal measure of land for aquatic purposes, with an extensive 160 million acres set aside for water management infrastructure. Different types of land resources are unevenly distributed in Shandong Province, forming a relatively complex land use pattern.

3. Data sources and research methods

3.1. Data source

Land use data used in this article are from ESA Sentinel-2 10m resolution imagery. (<https://livingatlas.arcgis.com/landcover/>); GDP, population and DEM data come from the Resource and Environmental Science and Data Center (<https://www.resdc.cn/>); precipitation and potential evapotranspiration data come from ERA5-Land (<https://cds.climate.copernicus.eu/>); soil database (HWSD) data come from the Earth Resources Data Cloud Platform (www.gis5g.com); vector data such as rivers, roads and county government locations at all levels come from Open Street Map (<https://www.openstreetmap.org>); evapotranspiration data in the future period come from China's 1km multi-scenario monthly potential evapotranspiration dataset;[8]Precipitation data in the future period comes from China's 1km resolution multi-scenario and multi-model Monthly precipitation data set.[9]

3.2. Research methods

3.2.1. PLUS model

The PLUS model determines the optimal land use layout and simulates future land use changes through the LEAS (land expansion analysis strategy) and CARS (CA based on multiple random seeds) modules. During the simulation process, it can explore the mechanism of land use change and fill the gaps in urban development. Modelling needs for spatial planning policies to guide land use change.[10] Its simulation results can better support the prediction of water yield assessment in the future period.

(1) LEAS parameter setting. The chosen approach for data collection employs a random sampling technique with a rate of 1%, mTry specified as 12, and it involves generating 20 decision trees. This process is executed using 8 parallel threads. The variables influencing the model include proximity to primary rivers, Digital Elevation Model (DEM), distance to prefectural cities, Gross Domestic Product (GDP), proximity to roads, population density, distance to fourth-order rivers, land gradient, ambient temperature, railway proximity, soil classification, and data on soil degradation.

(2) CARS simulation parameter settings. By default, the domain spans three units, the patch generation's attenuation factor decreases with a baseline of 0.5, the spread rate is established at 0.5, and there is a standard 5% chance for the initiation of random patch seeds.

(3) Transfer matrix setting. In the transfer matrix, 0 means that the transformation cannot take place and 1 means that the transformation can take place. Since the water area is a limiting factor, the water area can only be expanded without conversion. Building land is not easily converted to water, so it is set to No conversion to water.

(4) Setting neighbourhood weight parameters. The value range of neighbourhood weight is 0~1. The larger the value, the greater the influence of the neighbourhood, i.e. the stronger the expansion ability of the land type. This study is based on the land use data of 2017 and 2022, and calculates its expansion intensity according to the neighbourhood weight parameter method. Specifically, the neighbourhood weight parameters are shown in Table 1.

$$W_i = \frac{T_{Ai} - T_{Amin}}{T_{Amax} - T_{Amin}} \quad (1)$$

In the formula: W_i is the weight of land use type i and T_{Ai} is the area of land use type i expansion.

Table 1. Domain weight parameter settings

parameter	farmland	woodland	grassland	water	construction land	unused land
Weights	1	0.145	0.037	0.128	0.763	0

3.2.2. InVEST model annual water yield module

The formula to determine the water yield involves deducting the measured actual evapotranspiration from the projected rainfall for every individual grid section.

$$Y_x = \left(1 - \frac{AET_x}{P_x}\right) \times P_x \quad (2)$$

Within the equation, Y_x signifies the yearly hydrological output from a specified grid cell x ; AET_x denotes the grid cell's x yearly realized evapotranspiration; P_x indicates the yearly rainfall for grid cell x ; The computation of $\frac{AET_x}{P_x}$ within the equation employs the Budyko hypothesis for water-energy balance.

$$\frac{AET_x}{P_x} = \frac{1 + \omega_x R_{(x,j)}}{1 + \omega_x R_{(x,j)} + 1/R_{(x,j)}} \quad (3)$$

In the formula, $R_{(x)}$ is the dimensionless drying index of grid unit x ; ω_x is a dimensionless non physical parameter representing soil properties under natural climate conditions, defining a curve shape related to potential evapotranspiration

$$R_x = \frac{K_c \times ET_{0x}}{P_x} \quad (4)$$

$$\omega_x = Z \frac{AWC_x}{P_x} \quad (5)$$

Within the equation, the term K_c denotes the crop's coefficient for evapotranspirative processes; ET_{0x} corresponds to the baseline evapotranspiration for a given grid cell x ; Z stands for a derived coefficient, alternatively termed a "seasonal constant," that encapsulates the local precipitation patterns and additional hydrogeological factors, typically fluctuating between 1 and 30; AWC_x signifies the water content within the plant matter (measured in millimeters), with the following computational expression:

$$AWC_x = \min(\text{soil_depth}, \text{root_depth}) \times PAWC \quad (6)$$

Within the equation, 'soil_depth' represents the thickness of the soil layer, 'root_depth' refers to the length of the roots, and 'PAWC' denotes a curve-fitting model derived from the properties of soil texture and organic content, which facilitates plant water usage, The value range is 0-1.

$$PAWC = 54.509 - 0.132 \times \text{Sand\%} - 0.003 \times (\text{Sand\%})^2 - 0.055 \times \text{Silt\%} - 0.006 \times x(\text{Silt})^2 - 0.738 \times \text{Clay\%} + 0.007 \times (\text{Clay\%})^2 - 2.688 \times \text{OM\%} + 0.501 \times x(\text{OM\%})^{2[11]} \quad (7)$$

Within the equation, the symbol Sand% signifies the proportion of sand particles in the soil; Silt% denotes the proportion of fine soil particles present; Clay% corresponds to the amount of clay particles in the soil; and OM% reflects the percentage of organic matter within the soil.

The evapotranspiration data was obtained using the Hargreaves potential evapotranspiration calculation formula,[8] which is as follows:

$$PET = 0.0023 \times S_0 \times \text{Sqrt}(\text{MaxT} - \text{MinT}) \times (\text{MeanT} + 17.8) \quad (8)$$

Within this context, 'PET' denotes the estimated evapotranspiration with units in millimeters per month; 'MaxT', 'MinT', and 'MeanT' correspond to the monthly maximum, minimum, and mean temperatures, in that order; whereas 'S₀' represents the calculated theoretical solar irradiance at the Earth's atmospheric boundary, which is determined by accounting for the solar constant, Earth-Sun separation, Julian date, solar declination, and additional variables.

3.2.3. Global correlation analysis

Within the sphere of worldwide correlation studies, Moran's I often serves as the prevalent statistical indicator for spatial autocorrelation, a tool frequently employed in both geographical and statistical evaluations. Its primary function is to quantify the typical level of association among all the spatial entities within a given territory and their adjacent zones. The equation is presented below.

$$I = \frac{n \sum_{i=1}^n \sum_{j \neq 1}^n W_{ij} (x_i - \bar{x})(x_j - \bar{x})}{s^2 \sum_{i=1}^n \sum_{j \neq 1}^n w_{ij}} \quad (9)$$

$$I_i = \frac{(x_i - \bar{x})}{s^2} \sum_j W_{ij} (x_j - \bar{x}) \quad (10)$$

Within the equation, 'I' denotes the global spatial autocorrelation coefficient, while 'I_i' indicates the corresponding local spatial autocorrelation coefficient for each area; 'n' stands for the total count of geographical units; 'x_i' and 'x_j' refer to the data points for individual samples i and j in turn, with 'x' being the mean value across all samples; the matrix 'W_{ij}' embodies the weights assigned to spatial interactions among these units.

4. Analysis

4.1. Land use change in Shandong Province

Land use in Shandong Province is mainly focused on arable land, followed by construction land and grassland. Between 2017 and 2022, data from Figure 1 illustrates notable transformations in how land was utilized within Shandong Province. There was a measurable contraction in the expanse of arable land, dropping by 6.56% from 93,041.47 square kilometers to 86,916.08 square kilometers. Meanwhile, forested regions expanded by a noteworthy 35.29%, increasing from 2,946.74 square kilometers to 3,987.88 square kilometers. The grassland area decreased slightly from 15986.16 square kilometers to 15591.06 square kilometers, a decrease of 2.46%. Over the past five years, the water area has also increased by 9.99%, from 9430.59 square kilometers to 10371.46 square kilometers, mainly due to the government's significant achievements in water resource protection and water environment management. Furthermore, as urbanization hastens, the need for land designated for city building persists in its upward trajectory; the expanse allocated to construction surged from 36,113.21 square kilometers to 40,828.14 square kilometers, marking a 13.05% climb. Concurrently, efforts to develop and exploit previously untouched land magnified, enhancing the efficiency of land resource use. Consequently, the extent of land remaining unutilized shrank from 393.52 square kilometers to 217.07 square kilometers, representing a substantial reduction of 44.89%. Table 2 displays the conversion matrix for various categories of land utilization

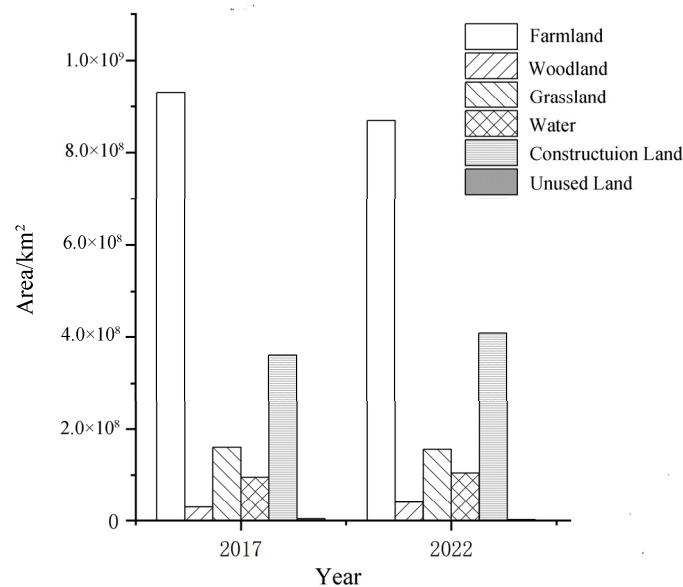


Fig. 1 Changes in Land Use Types

Table 2. Land Use Type Transfer Matrix in Shandong Province from 2017 to 2022 (km²)

Year/Land Use Type	2017						total	
	farmland	woodland	grassland	water	construction land	unused land		
2022	farmland	81376.39	499.09	2967.56	1289.43	5659.54	10.13	91802.14
	woodland	83.40	2309.12	456.94	15.65	42.31	0.07	2907.49
	grassland	2081.03	1065.45	11347.27	324.75	938.72	16.01	15773.22
	water	449.79	12.85	199.05	8395.79	178.22	69.27	9304.97
	construction land	1734.15	46.95	307.68	137.87	33385.50	20.04	35632.18
	unused land	33.59	1.31	104.88	69.83	80.02	98.65	388.28
	total	85758.34	3934.76	15383.38	10233.31	40284.30	214.18	155808.28

4.2. Temporal and spatial variability patterns of water production within the research zone

Annually, the InVEST water yield tool assesses Shandong Province's water output for the years 2017 through 2022, using the comprehensive water resource metrics and calibration model for water yields

as reported in the Shandong Provincial Water Resources Bulletin, with 2017 serving as the reference year and relying on genuine data from the same bulletin. After checking the Z parameter, after many tests, it was concluded that when the Z value is 8.8, the simulation effect is the best. From 2017 to 2022, the average precipitation increased from 640.21 mm to 818.79 mm, showing an upward trend with large inter-annual changes. Among them, 2020 to 2022 are wet years with large annual precipitation and water yield, and the maximum water volume is $6.83 \times 10^{10} \text{m}^3$ in 2021. 2017 and 2019 are dry years and the water yield is small. In 2019, the lowest recorded volume was 19.3 billion cubic meters. There exists a directly proportional relationship among rainfall, the amount of water yield, and the depth of water yield, with rainfall serving as the primary influential element. [6] During the same period, potential evapotranspiration showed a relatively stable state with small fluctuations. The maximum value occurred in 2019, which was 590.55 mm. Potential evapotranspiration affected water yield to some extent, and also affected groundwater recharge and consumption, but its impact may not be as pronounced as precipitation. Regarding the geographical extent, the production of water within the examined region diminishes moving from the southeast toward the northwest. Weihai, Rizhao and Qingdao have large water yield and water yield depth, which is much higher than inland cities such as Heze, Liaocheng and Dezhou. Given that coastal regions usually experience greater precipitation compared to their inland counterparts, the proximity of Weihai, Rizhao, and Qingdao to the sea means they are affected by maritime weather conditions. Rainfall is relatively abundant. At the same time, the terrain is less undulating, and precipitation can penetrate the soil better. Groundwater recharge is increased. In contrast, Heze, Liaocheng and Dezhou are located inland, with relatively low rainfall, highly undulating terrain and difficulty in percolating surface water, resulting in relatively low water yield.

4.3. Forecast of land use and water yield in Shandong Province

Based on the PLUS model and 12 influencing factors, taking the land use in 2017 as a benchmark, the land use test in 2022 shows that the kappa coefficient is 0.798287 and the overall accuracy is 0.878624. The accuracy test results are feasible and can be used for simulation forecasts and predictions for 2032. Land use in Shandong Province (Figure 2). From 2022 to 2032, the area of cultivated land in Shandong Province is predicted to decrease by 15524.0107 square kilometers (a decrease of 16.92%), the area of forest land will increase by 2352.9155 square kilometers, the area of grassland will decrease by 814.1342 square kilometers, the area of water will increase by 2204.277 square kilometers, and the area of construction land will increase by 12093.0404 square kilometers (an increase of 33.92%). The area of utilised land will decrease by 386.5657 square kilometers (Fig. 3).

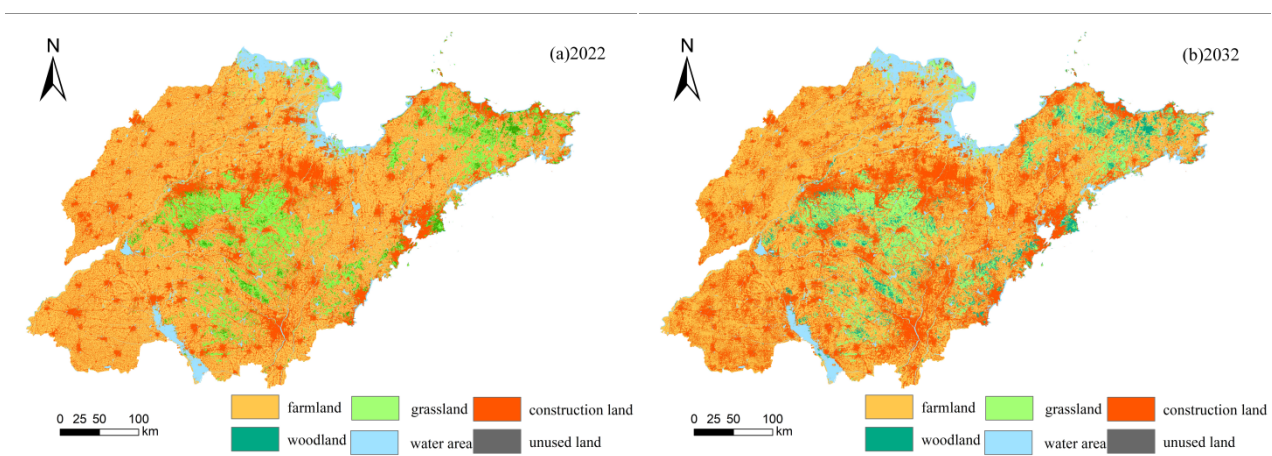


Fig. 2 Spatial distribution of land use types in Shandong Province in different years

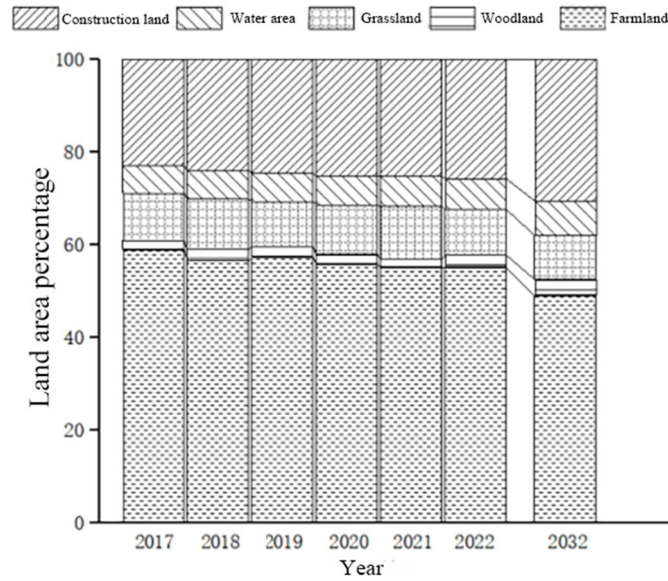


Fig. 3 Proportion of land use area in Shandong Province in different years

Based on the latest SSP (Shared Socioeconomic Pathways) scenario published by the IPCC, the precipitation and potential evapotranspiration data of three scenarios in 2032: very low forcing scenario (SSP119), medium forcing scenario (SSP245) and high forcing scenario (SSP585) are based on actual situation adjustment parameters and projected water yield data for three scenarios. The data over the years show that water yield and water depth are influenced by many factors and vary greatly from year to year. Precipitation and land use are the main influencing factors [6] For example, 2020 to 2022 will be a typical wet year with higher precipitation, higher regional water yield and higher water yield depth. In the SSP119 scenario, the water yield is relatively high and the water yield depth is large. Its change trend is similar to that of precipitation, and precipitation and evapotranspiration are generally higher than in the other two scenarios. Under the SSP245 scenario, the average water yield and water yield depth are relatively low, and the water yield and precipitation are between SSP119 and SSP585. Water yield, precipitation and evapotranspiration are generally lower under the SSP585 scenario. (Table 3).

Table 3. water yield in Shandong Province over the years

Year/scene mode	Annual precipitation(mm)	Potential evapotranspiration(mm)	Water yield($10^{10}m^3$)	Water yield depth(mm)
2017	640.21	586.15	2.70969	176.5
2018	798.22	573.39	4.76657	310.4
2019	561.62	590.55	1.93321	125.9
2020	889.09	568.74	6.16049	401.2
2021	943.39	569.35	6.82821	444.7
2022	818.79	579.14	5.08568	331.2
SSP119	693.48	576.62	3.64019	230.8
SSP245	672.01	615.72	3.23016	205.1
SSP585	586.84	624.38	2.20385	137.9

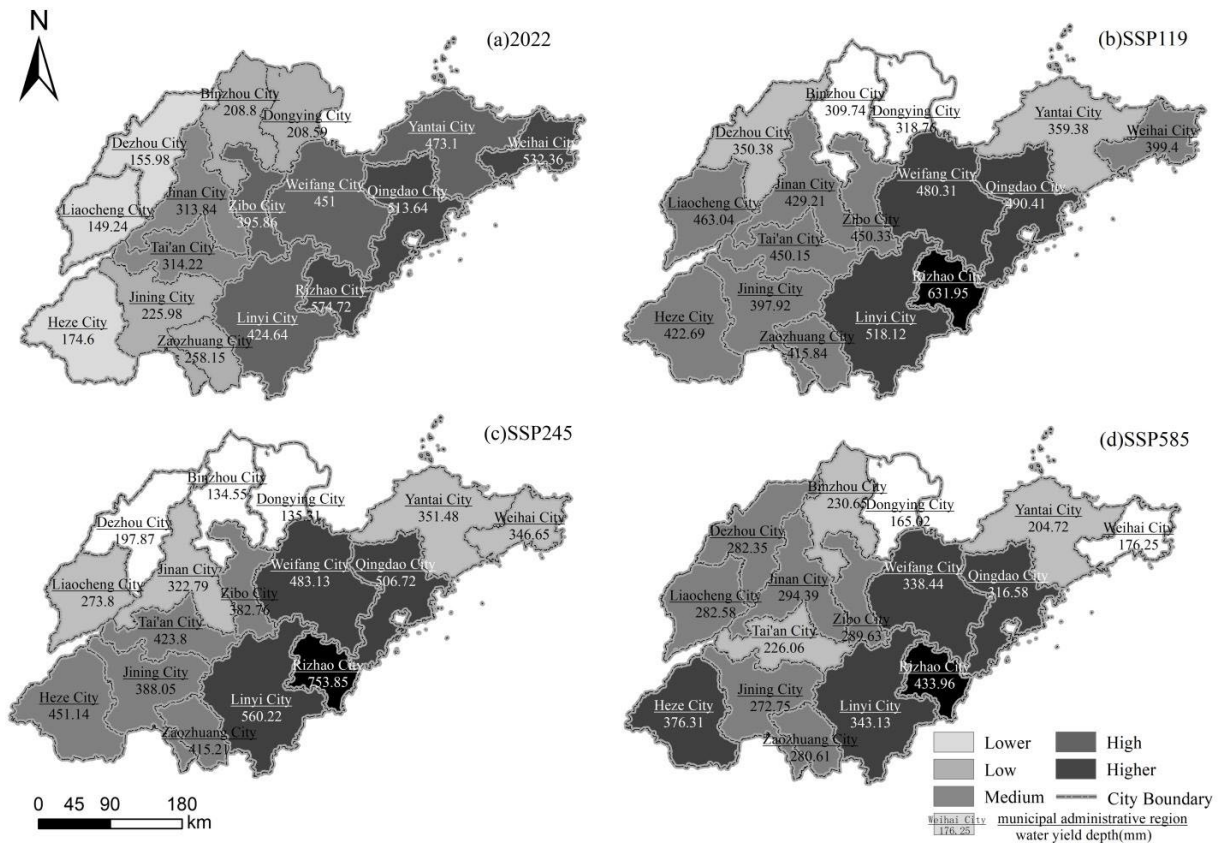


Fig. 4 Spatial distribution of water yield depth in Shandong Province in different years

Based on the above prediction results and comparing different scenarios, the water yield under each scenario is shown in Fig. 4, which is divided into five levels according to the different degrees of water yield depth. There are certain differences in the spatial distribution of water yield under different scenarios. In SSP119 and SSP245, the water yield depth decreases from southeast to northwest. SSP119 water yield depth and water yield volume are larger compared to other scenarios. The distribution of water yield depth in the SSP585 scenario is relatively fragmented, showing clustering in the southeast and discrete distribution in other areas. In all three scenarios, the water yield depth in offshore areas is larger than that in inland areas, with Rizhao having the largest water yield depth and Binzhou and Dongying having the smallest water yield depth.

4.4. Spatial autocorrelation analysis

The global Moran's I index of SSP119, SSP245 and SSP585 in 2022 and 2032 is 0.343, 0.275, 0.397 and 0.258 respectively. At this point in time, $P=0.001$ is much less than 0.05 and Moran's I is considered significant. The local spatial autocorrelation clustering plot is shown in Fig. 5. According to different scenarios, differences in precipitation and evapotranspiration, the clustering diagram and water yield depth show certain similarities. Among them, the HH clustering areas are mainly reflected in the southeast of Shandong Province, such as Rizhao City and Linyi City, as well as parts of Qingdao City and Weifang City, the proportion of 18.70% in 2022 will be reduced to 7.79%, 13.74%, 6.82% according to different scenarios. The LL agglomeration area is mainly reflected in the northern part of Shandong Province. From 2022 to 2032, the proportion of LL agglomeration area will be reduced from 18.75% in 2022 to 9.51%, 15.74% and 11.88% according to different scenarios, from the west to the northwest region. The north-east region migrates and the original LL spatial autocorrelation becomes LH or insignificant.

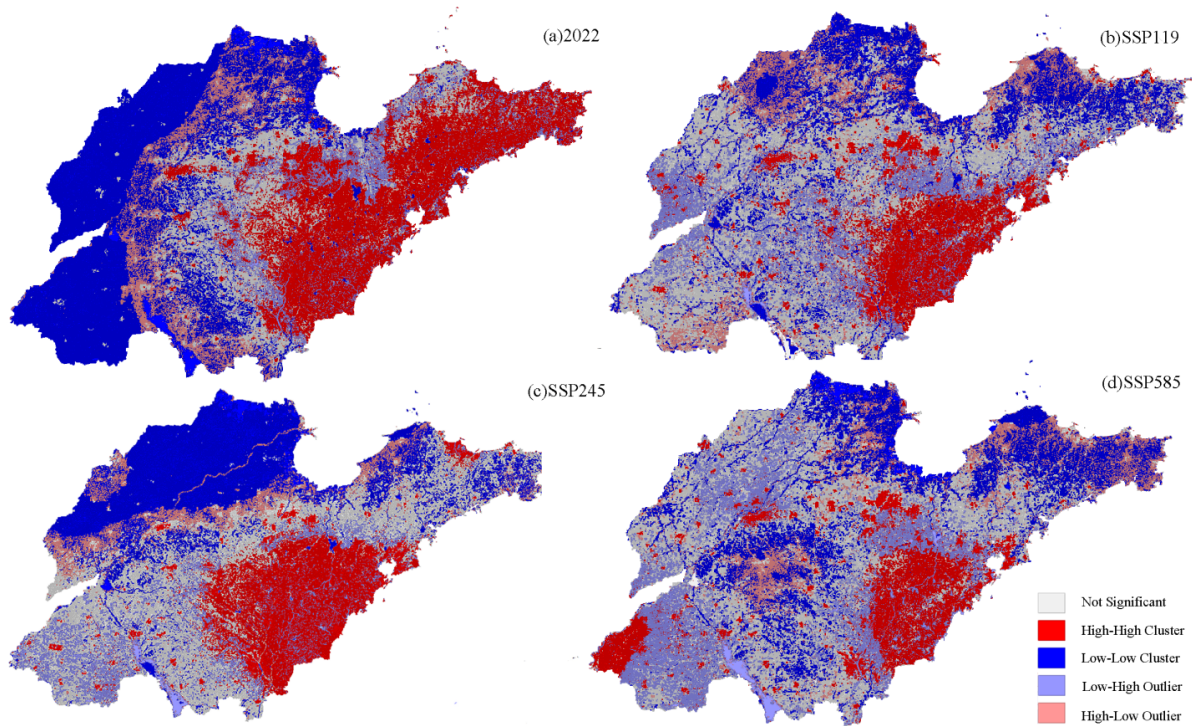


Fig. 5 Moran aggregation diagram

5. Conclusion

(1) The main characteristics of land use changes in Shandong Province from 2017 to 2022 are: the area of cultivated land decreases, the area of forest and water areas increases, the area of grassland is relatively stable, and the area of construction land and unused land both decrease to varying degrees. Among them, the changes in cultivated land and construction land are the most obvious, followed by water areas, which represent the significant results of the acceleration of urbanisation in Shandong Province and the protection of water resources and environmental management.

(2) From 2017 to 2022, water yield in Shandong Province will show certain spatial and temporal changes. Precipitation is highly variable and inter-annual changes have a significant impact on water yield. Potential evapotranspiration shows a relatively stable state with small fluctuations. Factors such as precipitation and potential evapotranspiration affect not only water yield, but also groundwater recharge and consumption. During the same period, water yield fluctuated significantly with large inter-annual variations and showed some correlation with precipitation and potential evapotranspiration. In terms of spatial distribution, water yield decreases from southeast to northwest, with higher water yield in coastal cities and lower water yield in inland areas. On the one hand, the degree of development and use of water resources in coastal areas is usually high, including the construction of reservoirs, artificial water diversions and groundwater extraction, which help to improve the availability of local water resources and thus increase water yield. In contrast, the development and use of water resources in inland areas may be relatively low. On the other hand, according to land use analysis, coastal areas tend to have higher vegetation cover, which can slow surface runoff and increase rainwater infiltration, thereby increasing water yield. Inland areas may have problems such as land degradation and low vegetation cover.

(3) Using the land use data from the PLUS model and the SSP scenario in the future, and predicted precipitation and potential evapotranspiration data for the same period, water yield is calculated using the InVEST water yield module. Under the SSP119 scenario, the precipitation is higher and the water yield depth is relatively high. The water yield depth and precipitation under the SSP245 scenario are between SSP119 and SSP585. In the SSP585 scenario, the water yield depth is lower than in the other scenarios, the relative precipitation is slightly lower, the evapotranspiration is high and the water yield

depth distribution is fragmented. Due to various factors such as climatic conditions, topography, water resources development and use, land cover changes and socio-economic factors, different scenarios show a decrease from the south-east coastal direction to the north-west inland direction.

(4) The spatial distribution of water yield in Shandong Province in 2032 shows a certain positive spatial correlation. Except for insignificant areas, the spatial aggregation types are mainly L-L and H-H aggregation types. In 2032, L-L aggregation occurs in the SSP119, SSP245 and SSP585 scenarios. Compared to 2022, the districts have decreased by 9.24%, 3.01% and 6.88% respectively, while the H-H cluster areas have decreased by 10.9%, 4.96% and 11.88% respectively compared to 2022.

Acknowledgements

Funding: This research was financially supported by the National Key Research and Development Program of China (2021YFC3200504, 2018YFC0408006, 2016YFC0402809), Key Hydraulic Engineering Research and Experiment Project for River Basin Water Conservancy Management and Service Center of Shandong Province (XQHfHZL-KY202004), Ministry of Water Resources' Special Funds for Scientific Research on Public Welfare (201401003), International Science and Technology Cooperation Program of China (2012DFG22140) and the Sub-project of National Science and Technology Major Project on Water Pollution Control and Treatment (2012ZX07404-003).

References

- [1] Cheng Xia, Jing Huilin, Lu Xiayi. Current Situation and Suggestions on Yellow River
- [2] Zheng Xu, Wei Leming, Guo Jianjun, et al. Analysis of Driving Forces of Water Yield in Inland River Basin in Arid Regions Based on Geographic Detector: A Case Study of Shule River Basin[J]. *Arid Land Geography*, 2020, 43(06): 1477-1485.
- [3] Zhang X, Chen X, Zhang W, et al. Impact of Land Use Changes on the Surface Runoff and Nutrient Load in the Three Gorges Reservoir Area, China[J]. *Sustainability*, 2022, 14.
- [4] Sun Qi, Xu Changchun, Ren Zhengliang, et al. Spatial-Temporal Distribution and Driving Factors Analysis of Water Yield in the Tarim River Basin[J]. *Journal of Irrigation and Drainage*, 2021, 40(08): 114-122. DOI: 10.13522/j.cnki.gggs.2020698.
- [5] Sun Yanwei, Li Jialin, Ma Renfeng, et al. Spatial Distribution Pattern of Water Supply Services in Yuqiao Reservoir Basin[J]. *Journal of Water Resources and Water Engineering*, 2015, 26(06): 1-6.
- [6] Lang W D X. Projected land use changes impacts on water yields in the karst mountain areas of China[J]. *Physics and chemistry of the earth*, 2018, 104.
- [7] Wu Jian, Li Yinghua, Huang Liya, et al. Spatial and Temporal Distribution Patterns of Water Yield in the Northeast Region of China and Its Driving Factors [J]. *Journal of Ecology*, 2017, 36(11): 3216-3223. DOI: 10.13292/j.1000-4890.201711.032.
- [8] Peng, S.Z., Ding, Y.X., Wen, Z.M., Chen, Y.M., Cao, Y., & Ren, J.Y. (2017). Spatiotemporal change and trend analysis of potential evapotranspiration over the Loess Plateau of China during 2011-2100. *Agricultural and Forest Meteorology*, 233, 183-194.
- [9] Peng, S.Z., Ding, Y.X., Liu, W.Z., & Li, Z. (2019). 1 km monthly temperature and precipitation dataset for China from 1901 to 2017. *Earth System Science Data*, 11, 1931–1946.
- [10] C X L A B , B Q G A , C K C C , et al. Understanding the drivers of sustainable land expansion using a patch-generating land use simulation (PLUS) model: A case study in Wuhan, China[J]. *Computers, Environment and Urban Systems*, 85[2024-01-26]. DOI:10.48550/arXiv.2010.11541., 2004, 21 (1):10.48550/arXiv.2010.11541.
- [11] Zhou Wenzuo. Study on Soil Available Water Content of Major Soil Types in China Based on GIS [D]. Nanjing Agricultural University, 2004.